Scale Effect on Recirculation Zone of the Bluff-body Burner with Concentric Jets

Jing-Tang Yang and Yu-Ping Kang

Department of Power Mechanical Engineering
National Tsing Hua University
Hsinchu, Taiwan 30043
E-mail: jtyang@pme.nthu.edu.tw

Turbulent non-premixed flame stabilized by bluff-body flame holders is often used in many practical combustion systems. The confined [1-2] and unconfined [3-5] reacting flow behind an axisymmetric bluff-body (e.g., discs, cones, or cylinders) has been extensively studied. Among various flame holders, the disc-type bluff-body burner with concentric jets usually generates a much stronger turbulent mixing and reaction compared to the burner with pure jet flame. Variations of the structure of the recirculation zone lead to major changes of flame patterns in flame-holding zone [6-7]; e.g., Yang *et al.* [6] identified five flame modes as the velocities of the air and fuel jets were systematically varied. Previous studies indicate that the geometry and inlet flow conditions of the bluff-body are two major factors that significantly affect the characteristics of the recirculation bubble. This paper, therefore, extends the preceding work in Ref. 6 and aims to explore the scale effect on recirculation zone of the bluff-body burner with concentric jets.

The schematic diagram of the experimental setup is sketched in Fig. 1. The test section consisted of a central-fuel jet and a concentric annular-air flow, separated by a disc-type bluff-body. The disc diameter D was variable between 25, 35, 45, 50 mm, while the inner diameter of the annular air tube D_a was kept constant at 55.1 mm. The corresponding air flow blockage ratios (BR), defined as $(D/D_a)^2 \times 100\%$, were 21%, 40%, 67%, and 82%, respectively. Three layers of stainless steel mesh upstream in the annulus inlet straightened the air flow. The central tube was 60 cm long and 3.5 mm in inner diameter (l/D_f ~170) to ensure a fully developed turbulent pipe flow at burner exit. The fuel supply was connected directly to commercial grade propane gas (95% C_3H_8, 3.5% C_2H_6, and 1.5% C_4H_{10}). The burner was placed in a still-air environment and protected with a fine-wire mesh screen from any outside flow disturbance. Schlieren optical technique was employed to observe the combusting flow field by the first-order density variation. Mean temperature was measured by an R-type thermocouple with diameter 125 μm. Fluorescence images of the hydroxyl radical, excited with a planar laser-induced fluorescence spectroscopy (PLIF), were used to probe the reacting feature of the non-premixed flame.

Besides the flame blow-out, the flame was classified into five distinct modes: (I) recirculation flame, (II) central-jet dominated flame, (III) jet-like flame, (IV) partially quenched flame, and (V) lift-off flame, as shown in Fig. 2. Figures 3 and 4 show the combustion regime diagrams, which were established by adjusting the fuel-to-air velocity ratio (γ) and the fuel-to-air momentum ratio (MR) for four air flow blockage ratios. The transition from jet-like

flame to lift-off flame was obviously highly sensitive to the blockage ratio. The jet-like flame became more and more unstable when the blockage ratio was increased from 67% to 82%. The range of the annular-air velocity/momentum corresponding to the lift-off flame broadened with the increasing blockage ratio. However, the central-fuel velocity corresponding to the blow-out limit remained at 60 m/s whereas the blockage ratio altered between 21% and 67% and began to decreased once the blockage ratio exceeded 67%.

Figure 5 shows the photographs of flame structures of the central-jet dominated flame mode corresponding to four blockage ratios at γ = 1.74 (U_f = 9.60 m/s, U_a = 5.51 m/s). Since the momentum of fuel-jet was large relative to the air jet, the fuel-jet penetrated through the recirculation zone and a blue flame occurred in the blue-neck region, which connected a downstream yellow flame to the recirculation zone flame. At BR = 21%, the flame structure was similar to the diffusion jet flame. The flame configuration on the recirculation was more obvious as the blockage ratio got larger. The instantaneous Schlieren photographs (Fig. 6) corresponding to Fig. 5 contained an apparently black demarcation line outside the recirculation zone and revealed the temperature gradient was high herein. Moreover, the part of the central jet was more blackish relative to inside of the recirculation zone, implying that there was a high temperature difference between both regions.

Figures 7 and 8 represent the distribution of mean temperature at γ = 0.75 (U_f = 4.58 m/s, U_a = 6.08 m/s) and γ = 1.74 (U_f = 9.60 m/s, U_a = 5.51 m/s), respectively. At γ = 0.75, the highest temperature was located around the outer shear layer. Since the fuel-jet penetrated the recirculation zone, some fresh penetrating fuel mixed with the burnt gas which did not be embroiled in the recirculation zone and would be pulled downstream to form another high temperature region. As shown in Fig. 7, the high temperature region heightened with the decreasing blockage ratio. While γ varied from 0.75 to 1.74, the central fuel-jet not only penetrated the recirculation zone but also overcame completely the backflow momentum of air-driven vortex. Although, the temperature of the central jet in recirculation zone was still low, the high temperature on the outer shear layer of air-driven vortex moved to upstream and filled with inside of recirculation zone. This phenomenon was more noteworthy as the blockage ratio got larger.

The fluorescence images of hydroxyl radicals in Figs. 9 and 10, contrasting respectively the distribution of mean temperature in Figs. 7 and 8, show the similarity between the thermal structure and combustion zone. Since the time scale of heat transfer exceeds the life time of the hydroxyl radicals, the thermal zone has a wider distribution. At γ = 0.75, the main combustion zone occurred around the parts of the recirculating vortex and the central jet closed to the blue-neck region, where the fuel-jet and the large-scale motion of the entrained air interacted mutually. As the fuel-to-air velocity ratio raised to 1.74, the main combustion zone moved gradually toward the inner side of the recirculation zone and the OH signal intensity turned weaker.

The fluorescence images of hydroxyl radicals in Fig. 11 were taken with a constant annular air velocity 6.08 m/s to expose the transition of the OH zone under the influence of various of blockage ratios and fuel-to-air velocity ratios. The blockage ratio and velocity ratio are both the important factors to induce the change of the high temperature reaction zone. While the blockage

ratio got larger, the main combustion zone also moved regularly toward the inner side of the recirculation zone and the hydroxyl radical signal intensity became powerless, just as that of increasing fuel-to-air velocity ratio. With a constant γ, the reverse momentum of air-driven vortex decreases as the blockage ratio increases. The recirculating vortex moving forward to upstream near the disc would be easily induced to downstream by energetic central-fuel jet. Therefore, the combustion zone moved toward the low-velocity and long-detainment upstream of recirculation zone. Photographs in Fig. 12 illustrate the development of the OH zone with varied blockage ratios and fuel-to-air momentum ratios. The OH signal intensity of the central torch grew weaker while the fuel-to-air momentum ratio was heightened for any blockage ratio. The transition of combustion zone was apparently dominated by the momentum ratio.

References

1. Winterfeld, G. (1965). On Processes of Turbulent Exchange Behind Flame Holders. *10th Symp. (Int.) on Combustion*, The Combustion Institute, Pittsburgh, p. 1265.
2. Taylor, A. M. K. and Whitelaw, J. H. (1984). Velocity Characteristics in the Turbulent Near Wakes of Confined Axisymmetric Bluff Bodies. *J. Fluid Mech.*, **139**, 391.
3. Chigier, N. A. and Beer, J. M. (1964). The Flow Region Near the Nozzle in Double Concentric Jets. *Trans. ASME, J. Basic Engineering*, **86**, 797.
4. Davies, T. W. and Beer, J. M. (1970). Flow in the Wake of Bluff-Body Flame Stabilizers. *13th Symp. (Int.) on Combustion*, The Combustion Institute, Pittsburgh, p. 631.
5. Prade, B. and Lenze, B. (1992). Experimental Investigation in Extinction of Turbulent Non-Premixed Disk Stabilized Flames. *24th Symp. (Int.) on Combustion*, The Combustion Institute, Pittsburgh, p. 369.
6. Yang, J. T., Chang, C. C. and Lin, M. T. (1995). Effects of Central Jet Velocity on Non-premixed Flame of a Gas Burner with a Disc Stabilizer. *The 9th Congress and Exposition on Gas Turbines in Cogeneration and Utility*, Industrial and Independent Power Generation, Vienna, Austria, August 23-25, Paper 95-CTP-44.
7. Huang, R. F., Yang, J. T. and Lee, P. C. (1997). Flame and Flow Characteristics of Double Concentric Jets. *Combustion and Flame*, **108**, 9.

Figure captions

Fig. 1 Schematic diagram of the experimental apparatus.
Fig. 2 Photographs of the flame modes.
Fig. 3 Combustion regime diagram with varied central-fuel and annular-air velocity.
Fig. 4 Combustion regime diagram with varied central-fuel and annular-air momentum.
Fig. 5 Photographs of flame structures of the central-jet dominated flame mode, γ = 1.74; U_f = 9.60 m/s, U_a = 5.51 m/s.
Fig. 6 Schlieren photographs of the central-jet dominated flame mode, γ = 1.74; U_f = 9.60 m/s, U_a = 5.51m/s.
Fig. 7 Distributions of mean temperature, γ = 0.75;U_f = 4.58 m/s, U_a = 6.08 m/s.
Fig. 8 Distributions of mean temperature, γ = 1.74; U_f = 9.60 m/s, U_a = 5.51 m/s.
Fig. 9 Fluorescence images of hydroxyl radicals, γ = 0.75; U_f = 4.58 m/s, U_a = 6.08 m/s.
Fig. 10 Fluorescence images of hydroxyl radicals, γ = 1.74; U_f = 9.60 m/s, U_a = 5.51 m/s.
Fig. 11 Effect of blockage ratio and velocity ratio on OH zone transition at outlet annular-air velocity 6.08 m/s.
Fig. 12 Effect of blockage ratio and momentum ratio on OH zone transition at outlet annular-air momentum 0.02 N.

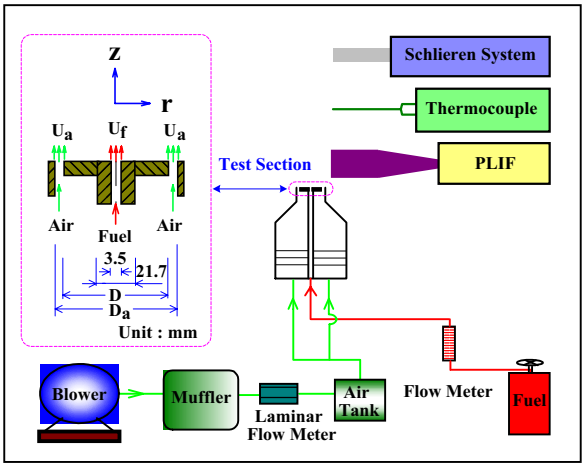

Fig.1

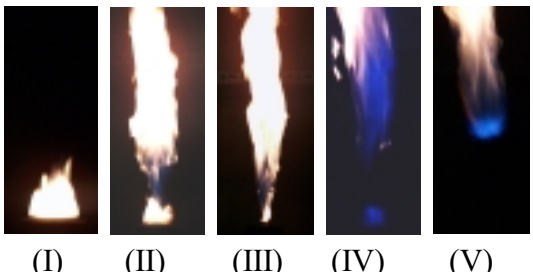

Fig.2

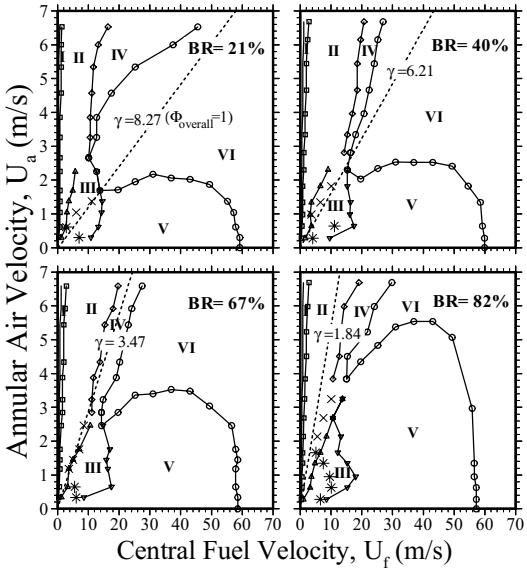

Regime I: recirculation zone flame.
Regime II: central-jet dominated flame.
Regime III: jet-like flame.
Regime IV: partially quenched flame.
Regime V: lift-off flame.
Regime VI: flame blow-out
＊: reattach
×: reattach blow-out

Fig.3

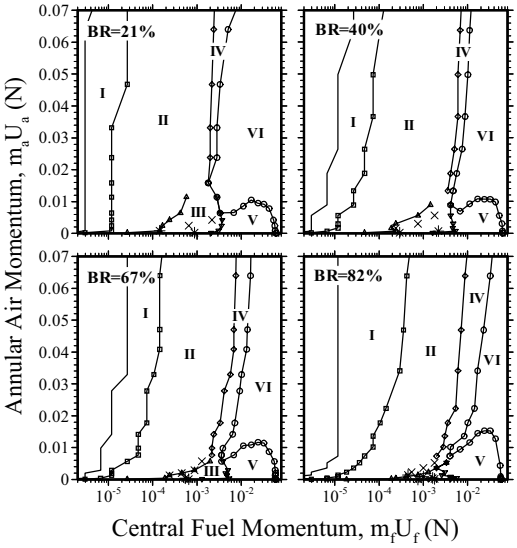

Fig.4

Fig.5

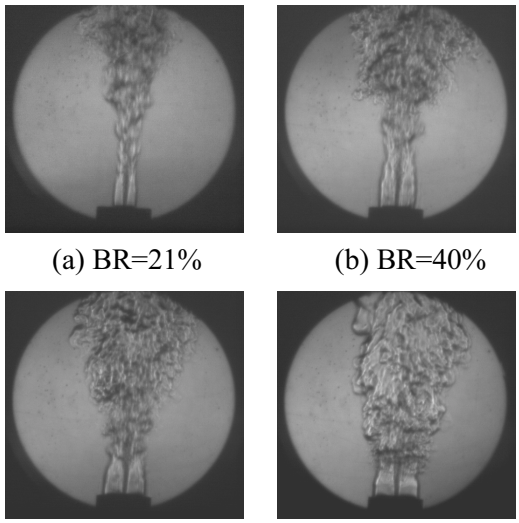

Fig.6

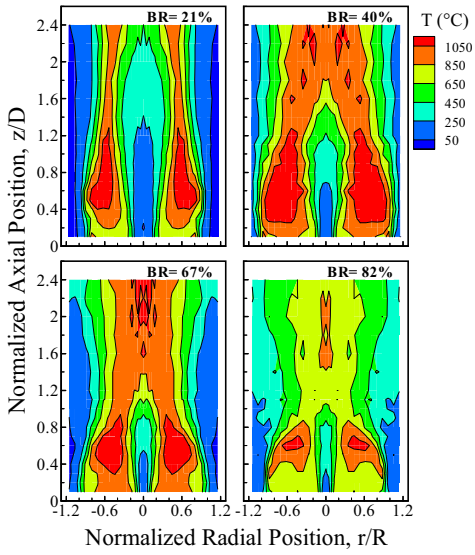

Fig.7

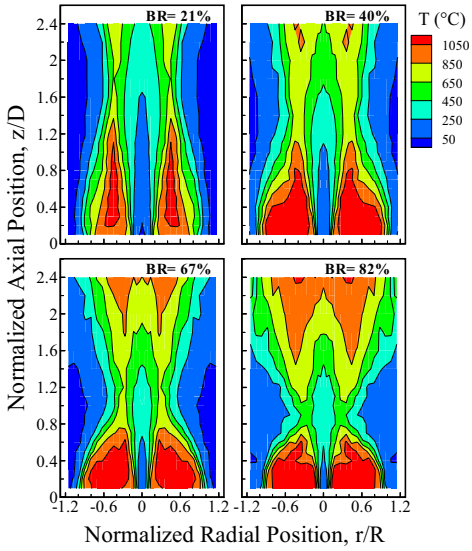

Fig.8

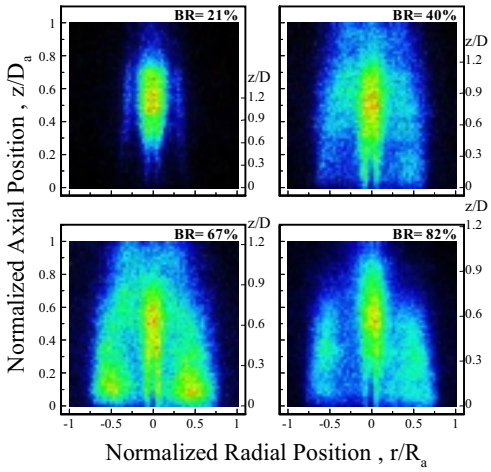

Fig.9

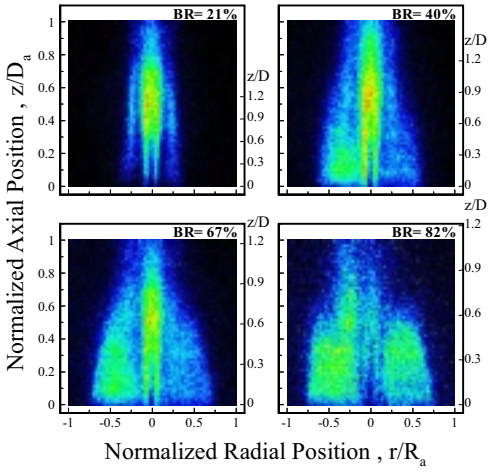

Fig.10

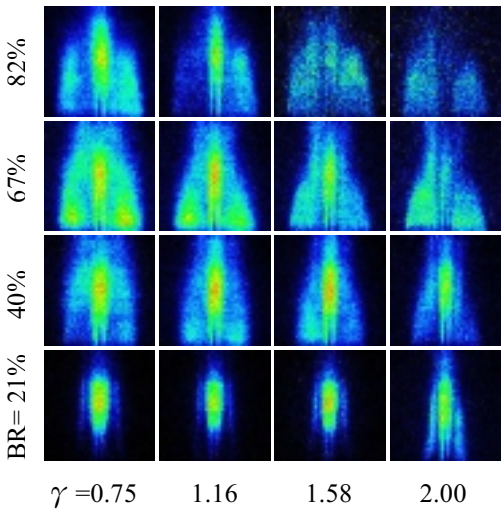

Fig.11

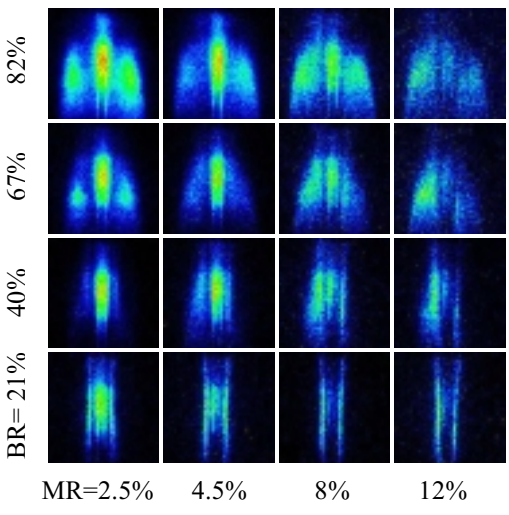

Fig.12